Since January 2020 Elsevier has created a COVID-19 resource centre with free information in English and Mandarin on the novel coronavirus COVID-19. The COVID-19 resource centre is hosted on Elsevier Connect, the company's public news and information website.

Virus Research 305 (2021) 198555

Contents lists available at ScienceDirect

Virus Research

journal homepage: www.elsevier.com/locate/virusres

Inactivation of SARS-CoV-2 by β-propiolactone causes aggregation of viral particles and loss of antigenic potential

Divya Gupta [a], Haripriya Parthasarathy [a], Vishal Sah [a,b], Dixit Tandel [a,b], Dhiviya Vedagiri [a,b], Shashikala Reddy [c], Krishnan H Harshan [a,b,*]

[a] Centre for Cellular and Molecular Biology, Hyderabad 500007, India
[b] Academy for Scientific and Innovative Research (AcSIR), Ghaziabad 201002, India
[c] Department of Microbiology, Osmania Medical College, Koti, Hyderabad 500095, Telangana, India

ARTICLE INFO

Keywords:
COVID-19
SARS-CoV-2
Virus inactivation
BPL
Antisera
Vaccine

ABSTRACT

Inactivated viral preparations are important resources in vaccine and antisera industry. Of the many vaccines that are being developed against COVID-19, inactivated whole-virus vaccines are also considered effective. β-propiolactone (BPL) is a widely used chemical inactivator of several viruses. Here, we analyze various concentrations of BPL to effectively inactivate SARS-CoV-2 and their effects on the biochemical properties of the virion particles. BPL at 1:2000 (v/v) concentrations effectively inactivated SARS-CoV-2. However, higher BPL concentrations resulted in the loss of both protein content as well as the antigenic integrity of the structural proteins. Higher concentrations also caused substantial aggregation of the virion particles possibly resulting in insufficient inactivation, and a loss in antigenic potential. We also identify that the viral RNA content in the culture supernatants can be a direct indicator of their antigenic content. Our findings may have important implications in the vaccine and antisera industry during COVID-19 pandemic.

1. Introduction

The ongoing COVID-19 pandemic caused by the coronavirus SARS-CoV-2 is devastating the human lives across the globe (Lu et al., 2020; Zhu et al., 2020). As of the middle of April 2021, the virus is estimated to have infected about 140 million people, killing over 3 million of them worldwide. The disease is characterized by acute respiratory illness resulting in severe breathing difficulties very similar to the common flu accompanied by severe cough in the infected people forcing several of them to be hospitalized. In addition, there have been several reports of sepsis, blood clotting, and multi-organ failure in several persons infected by the virus. The severity of the disease is significantly higher in persons with co-morbid conditions such as diabetes, hypertension, cancer, and respiratory problems (Zhu et al., 2020; Puelles et al., 2020). Currently, there are no drugs that can cure COVID-19. Vaccines are the best hopes for ending this pandemic. Antibody-based interventional therapies are of great importance in treating severe cases. Some of these projects utilize inactivated virus particles that are used for immunization along with adjuvants. Large-scale viral cultures and antigens are essential for successful generation of vaccines and antisera that are based on whole virus-derived antigens. This requires complete inactivation of the virus particles while causing minimum damage to their structural and antigenic properties. Therefore, these projects are dependent on the availability of viral samples that are totally inactivated while retaining their antigenicity sufficient to induce antibody response.

Several methods have been adapted historically to inactivate the viral stocks that are used for vaccine and antisera development. They include physical methods such as heat (Chen et al., 2020) and γ-rays (Furuya et al., 2010), or chemical agents such as formaldehyde and β-propiolactone (BPL) (Fan et al., 2017; Roberts et al., 2010; Patterson et al., 2020). SARS-CoV-2 is reported to be inactivated by temperatures starting from 56 °C (Jureka et al., 2020; Kariwa et al., 2004). BPL-mediated inactivation of SARS-CoV and SARS-CoV-2 has been demonstrated (Roberts et al., 2010; Jureka et al., 2020; See et al., 2008See et al., 2006). Heating is known to denature the proteins that might negatively impact their antigenicity (Chen et al., 2020). γ -irradiation has been employed in several vaccine studies, but they are also known to damage the antigens if not properly optimized (Kempner, 2001). Formaldehyde, despite being one of the oldest and most easily available chemical agents to inactivate viruses, also causes loss in

* Correspondence author at: Centre for Cellular and Molecular Biology, Hyderabad 500007, India.
E-mail address: hkrishnan@ccmb.res.in (K.H. Harshan).

https://doi.org/10.1016/j.virusres.2021.198555
Received 14 May 2021; Received in revised form 24 August 2021; Accepted 26 August 2021
Available online 4 September 2021

protein antigenicity and hence is less desirable. BPL has emerged as a very popular chemical agent in various vaccine initiatives due to its high inactivation potency and relatively low damage of antigens. BPL has also been used in SARS-CoV-2 inactivation at various concentrations. However, a comprehensive analysis of its potency and impact on the integrity of viral antigen is not available. In this study, we attempt to optimize the concentration of BPL for SARS-CoV-2 for efficient inactivation and protection of antigenicity. We demonstrate that BPL at 1:2000 concentrations (v/v) is enough to inactivate SARS-CoV-2 and increasing the BPL concentration above 1:1000 leads to significant drop in the antigenic potential of viral proteins, probably caused by the modifications on their amino acids. Our investigation also identified a lack of correlation between viral RNA titer and infectious viral units in the supernatant. However, the viral RNA titer showed strong correlation with the antigenic content in the sample. Our studies also demonstrate that SARS-CoV-2 particles tend to form larger aggregates with increasing concentrations of BPL above 1:1000 which could possibly lead to reduced epitope exposure thereby deleteriously affecting the antigenic potential of the sample.

2. Materials and methods

2.1. Cell culture and reagents

Vero cells were cultured in DMEM with 10% FBS (Hyclone, SH30084.03) and penicillin-streptomycin cocktail (Gibco, 15,140–122) at 37°C and 5% CO_2. Anti-Spike antibody was procured from Novus Biologicals (NB100–56,578) while anti-Nucleocapsid antibody was procured from Thermo Fisher (MA5–29,982). HRP-conjugated anti-rabbit secondary antibody was purchased from Jackson ImmunoResearch (111–035–003). BPL was procured from Himedia Laboratories (TC223–100). The zinc staining kit was from G Biosciences (Reversible Zinc Stain; 786–32ZN).

2.2. Virus culturing

All the experiments pertaining to the virus isolation and culturing were performed in the biosafety level-3 (BSL-3) laboratory at the Center for Cellular and Molecular Biology (CCMB). The oro- and nasopharyngeal patient swabs transported in virus transport medium (VTM) were screened using SARS-CoV-2 specific primers (LabGenomics; Labgun COVID-19 RT-PCR kit; CV9032B) and the samples with low Ct (less than 20) values were chosen to culture virus. VTMs were filter-sterilized and added to Vero monolayers in 96-well plate. Three hours post-infection, the media was replaced with fresh media. The infected cells were further incubated at 37 °C with 5% CO_2 in a humidified chamber and cytopathic effects (CPE) were examined every 24 h. Cells along with the supernatants were collected from those wells displaying CPE and transferred to fresh 12-well plate containing Vero monolayers for further propagation. This process was repeated until the cell culture supernatant showed a Ct value below 20. The supernatants were titrated for infectious particle count by plaque-forming assay. In the case of dry-swab sample, the swab was first soaked in Tris-EDTA (TE) buffer for 30 min (Kiran et al., 2020) and further stored at −80 °C. Later the sample was used as inoculum for infection similar to VTM.

2.3. Virus quantification, titration, and sequencing

RNA from VTMs or swab-immersed TE buffer or cell culture supernatant was isolated using viral RNA isolation kit (MACHEREY-NAGEL GmbH & Co. KG; 740,956.250). The SARS-CoV-2 RNA was quantified using (LabGun™ COVID-19 RT-PCR Kit) following the manufacturer's protocol or following WHO guidelines using SuperScript™ III Platinum™ One-Step qRT-PCR Kit (Thermo Fisher) and Taqman probes against CoV-2 E, and RdRP (Eurofins Scientific). The isolates that were established in cultures were sequenced by next-generation sequencing and compared with Wuhan SARS-CoV-2 genome as reference. The sequences of isolates used for all the experiments here were submitted to GISAID public database (GISAID ID: EPI_ISL_458,075; virus ID- hCoV-19/India/TG-CCMB-O2-P1/2020, and EPI_ISL_458,046; virus ID-hCoV-19/India/TG-CCMB-L1021/2020). Subsequently, the CCMB_O2 isolate was scaled up and used for the experiments. All the virus cultures were titrated for infectious particle count using plaque forming assay (PFU/mL) before use. Briefly, the supernatant was log-diluted from 10^{-1} to 10^{-7} in serum-free media and was added to a 100% confluent monolayer of Vero cells. Two hours post-infection the infection inoculum was replaced with agar media (one part of 1% low melting point agarose (LMA) mixed with one part of 2 × DMEM with 5% FBS and 1% Pen-Strep). 6–7 days post-infection, cells were fixed with 4% formaldehyde in 1 × PBS and stained with 0.1% crystal violet. The dilution which had 5–20 plaques was used for calculating PFU/mL. For RNase treatment, the supernatants were treated with 100 μg/mL of RNase A for 5 min after which they were separated for RNA preparation and plaque assays.

2.4. Virus infection and inactivation

Cells were infected with SARS-CoV-2 at 90% confluency in serum-free media at 1MOI for two hours and subsequently, the inoculum was replaced with fresh serum-free media. Three days post-infection, cell culture supernatant was collected, and the debris was removed by centrifugation and stored until further use. Later, the infectious viruses in the supernatants were inactivated using BPL at varying concentrations (1:250, 500, 1000, 2000 (v/v) to the culture-media). In brief, the supernatant with BPL was incubated at 4 °C for 16 h followed by 4-hour incubation at 37 °C to hydrolyze the remaining BPL. The inactivation of the virus was confirmed by the absence of CPE in three consecutive rounds of infections. To study the effect of BPL on viral antigenicity, either live infectious or inactivated viral samples were concentrated to 10 × using centrifugal filter units with 100 kDa cut-off.

2.5. Zinc staining

All the reagents provided by the manufacturer (Reversible Zinc Stain; G Biosciences) were diluted to working concentration using deionized water. Zinc staining was done after performing SDS-PAGE under reducing conditions. Viral supernatants either precipitated by ultracentrifugation, or concentrated by centrifugal filters were lysed with equal volume of 2 × lysis buffer (containing 2% NP40, 100 mM Tris–HCl, 300 mM NaCl, 2 mM sodium orthovanadate, 2 mM phenylmethylsulphonyl fluoride, 20 mM sodium pyrophosphate, and protease inhibitor cocktail) (George et al., 2012), mixed with 6 × Laemmli buffer, boiled and loaded onto the gels after cooling. Gels were washed with distilled water after electrophoresis followed by incubation in 25 mL washing buffer (Reagent I) for 5 min on a shaking platform. Subsequently, the gel was incubated with 25 mL of Reagent II containing imidazole for 15 min. Finally, the gel was stained in zinc sulfate-containing Reagent III for 45–60 s followed by immediate transfer to distilled water. The gel image was scanned against a dark background and was then destained using destaining solution provided by the manufacturer followed by three 5-minute washes using distilled water. The destained gel was used for subsequent western blot transfer procedures. Total protein content in each lane was quantified using ImageLab (Version 6; Bio-Rad) software and plotted against BPL dilutions.

2.6. Immunoblotting

Fresh gels or the destained gels after zinc staining were transferred onto PVDF membranes for 16 h at 30 V. Membranes were blocked in 5% BSA and were subsequently probed with SARS-CoV-2-specific Nucleocapsid (1:8000) or SARS Spike (1:2000) antibodies. HRP-conjugated

goat anti-rabbit secondary antibody was used at 1:20,000 dilutions. Blots were then developed with ECL reagents (Clarity ECL Western Blotting; Bio-Rad) using ChemiDoc MP system (Bio-Rad). All densitometric analyses were performed using ImageJ software (Schneider et al., 2012).

2.7. Dynamic light scattering spectroscopy (DLS)

The particle size of virions from BPL inactivated viral samples was measured using a dynamic light scattering instrument (SpectroSize 300; Nabitec). The instrument uses a laser diode and operates at a wavelength of 660 nm at 90° scattering angle and detection was done by an avalanche photodiode detector. Each BPL inactivated sample was subjected to twenty measurements to obtain the particle size. The data obtained was analyzed using SpectroSize 300 software that provided the average hydrodynamic size distribution profiles. The average size of the particles from each sample was plotted against the dilution of BPL used. Serum-free culture medium was used as the control for these measurements. The experiment was repeated in triplicate using samples with different Ct values.

2.8. Statistical analysis

Viral supernatants used in DLS assay were independently inhibited with BPL and were considered as biological replicates. At least three independent replicates were used to generate mean ± SEM, which are plotted graphically. Comparison was made with serum-free culture medium without viral particles that served as the control. To calculate statistical significance, two-tailed, unpaired student *t*-test was performed and the resultant *p* values were represented as *, **, ***, indicating *p* values ≤ 0.05, 0.005, and 0.0005 respectively.

3. Results

3.1. Establishment of SARS-CoV-2 cultures

Several other articles have described methods for the establishment of SARS-CoV-2 cultures (Kaye, 2006; Stelzer-Braid et al., 2020; Caly et al., 2020; Díaz et al., 2020). Here, the key is to have access to patient oro- or nasopharyngeal samples in viral transport medium (VTM) that display low Ct values in the quantitative real time RT-PCR assays. The association of the viral load estimated by qRT-PCR with COVID severity is controversial (Pujadas et al., 2020; Karahasan Yagci et al., 2020), and qRT-PCR-generated Ct values of viral genes are not true indicators of the viral load owing to a large number of variables in sample collection and processing and hence could be deceptive at times. Therefore, it is important to try several VTM samples that display Ct values below 30. Even though lower Ct values are indicators of high viral load in the sample, several samples with low Ct values could not establish infectivity in cell culture. This could primarily be determined by the infectious viral load in the sample that is dependent on the collection process and the post-collection storage conditions. Samples that did show signs of infection in a small scale (96-well set up) were then gradually expanded to larger scale to maintain a constant viral culture for further experiments. Each passage of virus was tested for viral load and titer to ensure the retention of infectivity (Table 1).

Recently, RNA extraction from the swab samples was shown to be dispensable thereby enabling direct processing of the samples for qRT-PCR in COVID-19 screening (Kiran et al., 2020), as well as in other respiratory viral infections (Borsanyiova et al., 2018; Moore et al., 2008). Collecting the samples in dry-swab form has been demonstrated to be effective in preserving the viral content and also much more bio-safe (Borsanyiova et al., 2018; Moore et al., 2008). The dry swabs were immersed in TE buffer before using directly in qRT-PCR. However, the dry-swab method has a potential risk of inactivating the virus due to long-term dry conditions. We tested if virus cultures can be established from the dry-swab samples resuspended in TE buffer stored at −80 °C. As in the case of VTM, the potential samples were incubated with Vero cells for infection. Interestingly, as demonstrated in Table 1, we successfully isolated SARS-CoV-2 from dry-swab collection sample, indicating that virus particles derived from dry-swab method can be viable and can indeed establish infection.

Table 1
Viral RNA contents and titers of three independent SARS-CoV-2 preparations isolated from patient swab samples and passage to larger formats. "P" indicates the passage number. The culture in which Vero cells were incubated with the patient sample was designated as P1. The third sample was isolated by the dry swab method as mentioned.

Isolate number	GISAID	Passage number	Ct value (E gene)	PFU/mL
1	EPI_ISL_458,075	P1	20.61	NA
		P2	17.34	3.14×10^{7}
		P3	19.01	1.57×10^{7}
2	EPI_ISL_458,046	P1	10.52	4.1×10^{7}
		P2	12.19	2.7×10^{7}
3 (Dry Swab)	NA	P1	20.95	NA
		P2	18.58	1×10^{4}
		P3	11.85	4.88×10^{6}

3.2. Ct values do not correlate with infectivity, but with protein content

Several studies have used Ct values as a measure of viral titer in the culture supernatants (La Scola et al., 2020; Kim et al., 2020). During our studies, we encountered numerous instances where low Ct values do not really translate into a high viral titer (Fig. 1A). Supernatants with Ct values differing significantly, displayed comparable viral titers. All these supernatants were harvested three days after the inoculation at about 30% CPE. We often came across samples with low Ct values and low infectious titers and also those with relatively higher Ct but with high viral titers. Large majority of the established culture supernatants had infectious titers around 10^7 PFU/mL but their Ct values ranged from 10 to 28, clearly pointing to a substantially large fraction of viral RNA contributed by non-infectious viral particles or non-virion associated viral RNA. We verified this possibility by treating three supernatants of known Ct values with RNase A for 5 min at room temperature followed by qRT-PCR and plaque assay. While RNase treatment significantly reduced the viral RNA content in the samples, as evident from the higher Ct values, the infectious titers were reduced only modestly, indicating that viral RNA from non-infectious viral particles contribute significantly to the RNA titer in the supernatant (Fig. 1B). However, samples with low Ct values corresponded to high viral protein content (Fig. 1C) suggesting that they contained larger amounts of defective and non-infectious viral particles that contributed to the higher protein content. Thus, the samples with low Ct values are ideal for the preparation of antigens irrespective of their infectious viral units.

3.3. Inactivation of SARS-CoV-2 by BPL

BPL is a common reagent used for chemical inactivation of viruses (Fan et al., 2017; Wiktor et al., 1972; Logrippo and Hartman, 1955). We titrated the optimal concentration of BPL required for inactivation of SARS-CoV-2. BPL was added to viral supernatants with known infectious titer (PFU/mL) to make final dilutions of 1:2000, 1:1000, 1:500 and 1:250 (all v/v). Infectivity of the supernatants was measured by CPE as described in the methods section. Our results demonstrate that BPL was consistently effective in inactivating the virus completely even at 1:2000 dilution, evident from the absence of plaque or cytopathic effect (Fig. 2B) unlike the untreated virus that showed clear plaques at higher dilutions (Fig. 2A). The inactivated viruses were passaged for three consecutive rounds to confirm the inactivation (Table 2). These results indicate that at 1:2000 concentration, BPL is strong enough to inactivate

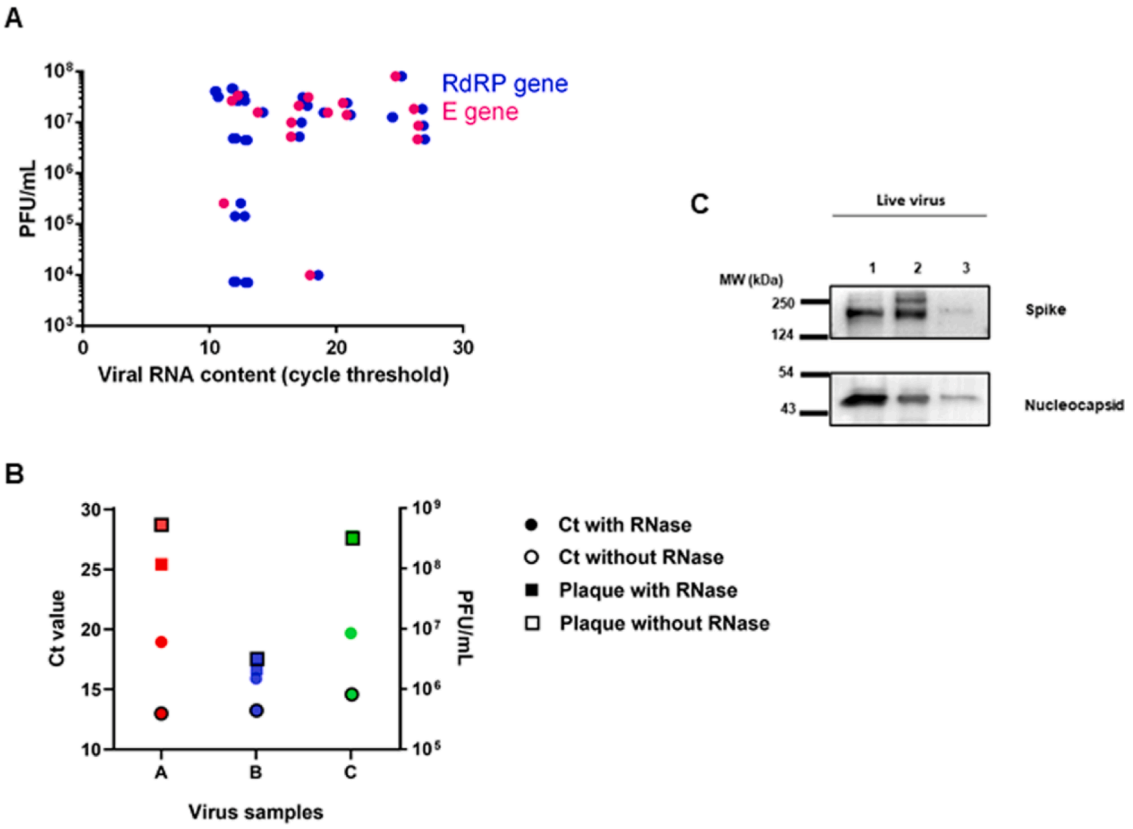

Fig. 1. RNA content of the virus cultures does not correlate with the infectious titers, but with the antigenic content. (A) Viral RNA content in cultures by qRT-PCR of E and RdRP genes were plotted against the infectious titers of the same cultures. RNA samples prepared from the supernatants were subjected to qRT-PCR for the detection of SARS-CoV-2 E and RdRP genes. Infectious titers of the cultures were determined by plaque forming assays. (B) Analysis of the RNase-susceptible, non-infectious fraction of the viral supernatants. Three independent viral supernatants of different Ct values were treated with 100 μg/mL of RNase A for 5 min along with appropriate control. Supernatants were divided for qRT-PCR and Plaque assay. Ct values and the infectious titers obtained from the RNase treated and untreated samples were plotted to generate the graph. (C) Analysis of the relative protein content of three viral supernatants with different viral RNA contents by immunoblotting of viral proteins. Sample 1, 2 and 3 had Ct values of 12.8, 14 and 17.7, respectively as determined by qRT-PCR of E gene. Immunoblotting was performed using specific antibodies.

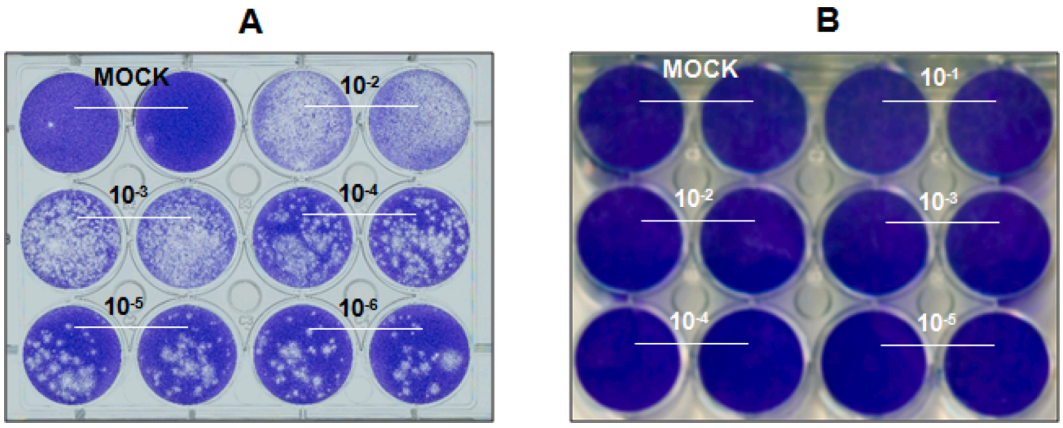

Fig. 2. Confirmation of the presence of infectious SARS-CoV-2 particles in the supernatant of the cultures. (A) Representative PFU assay plate showing consistent drop in the plaques with logarithmic dilution of the sample. (B) Confirmation of the inhibition of infectious virus particles with BPL treatment. Viral supernatant treated with BPL at 1:250 concentrations were inoculated with Vero cells and CPE was monitored for six days. Untreated supernatants were used in the control experiments. After six days, the supernatants were further inoculated with fresh cells and this was repeated for a third round of infection. The image is from the third round of repeated infection demonstrating the absence of CPE, confirming total inactivation of infectious virus particles.

SARS-CoV-2 efficiently.

3.4. BPL inactivation causes damage to SARS-CoV-2 antigens

One of the major requirements of BPL inactivation is in vaccine studies. However, BPL treatment consistently interfered with the quantification of viral protein. BPL is known to damage the genetic content, but its influence on the proteins of the virions is less understood (Perrin and Morgeaux, 1995). In addition, if BPL damages structural proteins of the virions, this could be less desirable for vaccine studies. To

Table 2
Demonstration of complete inactivation of virus particles by BPL after three rounds of consecutive culturing.

Sample ID	Before Inactivation		Inactivated virus infectious titer after three rounds of consecutive culturing			
	Ct (E gene)	Infectious titer (PFU/mL)	1:250	1:500	1:1000	1:2000
Sample 1	12.79	2.71×10^7	–	–	–	–
Sample 2	17.72	2.14×10^7	–	–	–	–
Sample 3	25.16	2.71×10^7	–	–	–	–

address this issue, we tested the epitope integrity of SARS-CoV-2 virions inactivated with BPL. Viral supernatants treated with BPL at 1:250 dilutions were concentrated 10 × by filters with 100 kDa cut-off membranes. Protein lysates prepared from these concentrates were electrophoresed by SDS-PAGE followed by zinc-staining to visualize and quantify the antigens. BPL treatment caused drop in the total protein content in the samples as demonstrated in Fig. 3A and B. Next, we studied the effect on antigenicity by detecting structural proteins spike (S) and nucleocapsid (N) by immunoblotting. Immunoblotting against S and N was used as a proxy measure of the antigenic integrity of the virions. Any drop in the band intensity would be considered as the outcome of potential damage to the epitopes. The immunoblots revealed a substantial loss of signals in BPL treated samples against the untreated, infectious samples (Fig. 3C and D), suggesting that BPL treatment is causing the loss of antigenic integrity in addition to causing loss in the protein content.

In order to further substantiate this point, we treated the viral supernatants with varying concentrations of BPL at 1:2000, 1:1000, 1:500 and 1:250 dilutions. Supporting our initial observations, loss in the signal was the most striking in sample with 1:250 BPL concentrations followed by 1:500 (Fig. 4A and B). BPL caused much less loss at 1:1000 and 1:2000 dilutions. This was further strengthened by immunoblotting where a gradual loss of antigenic integrity was remarkably captured in 1:250 dilutions (Fig. 4C). This could be caused either by a possible chemical modification of amino acids in the epitopes or by the potential loss of exposure of epitopes caused by aggregation. These results collectively demonstrate that BPL treatment causes loss in protein content and also a further loss in antigenicity, and suggest that using 1:2000 or 1:1000 dilutions would be more appropriate for vaccine production.

3.5. BPL treatment causes aggregation of SARS-CoV-2

Earlier studies have demonstrated that BPL treatment causes aggregation of virus particles (Fan et al., 2017). To test whether SARS-CoV-2 undergoes aggregation during BPL treatment, we used dynamic light scattering (DLS) that can study particle size distribution in a suspension. Viral supernatants treated with varying concentrations of BPL were analyzed by DLS. Interestingly, increasing concentrations of BPL induced the formation of larger aggregates as demonstrated in Fig. 5A–D. While the viral particles in the supernatant with BPL at 1:2000 dilutions had an average size of about 160 nm (in line with the size of a coronavirus particle of 120–160 nm), their size gradually increased to over 500 nm with 1:250 concentration of BPL (Fig. 5E). These results demonstrate that BPL causes aggregation of SARS-CoV-2 particles in a concentration-dependent manner.

Since various host proteins can associate with viral particles (Gale et al., 2019), such aggregation by BPL could further diminish the

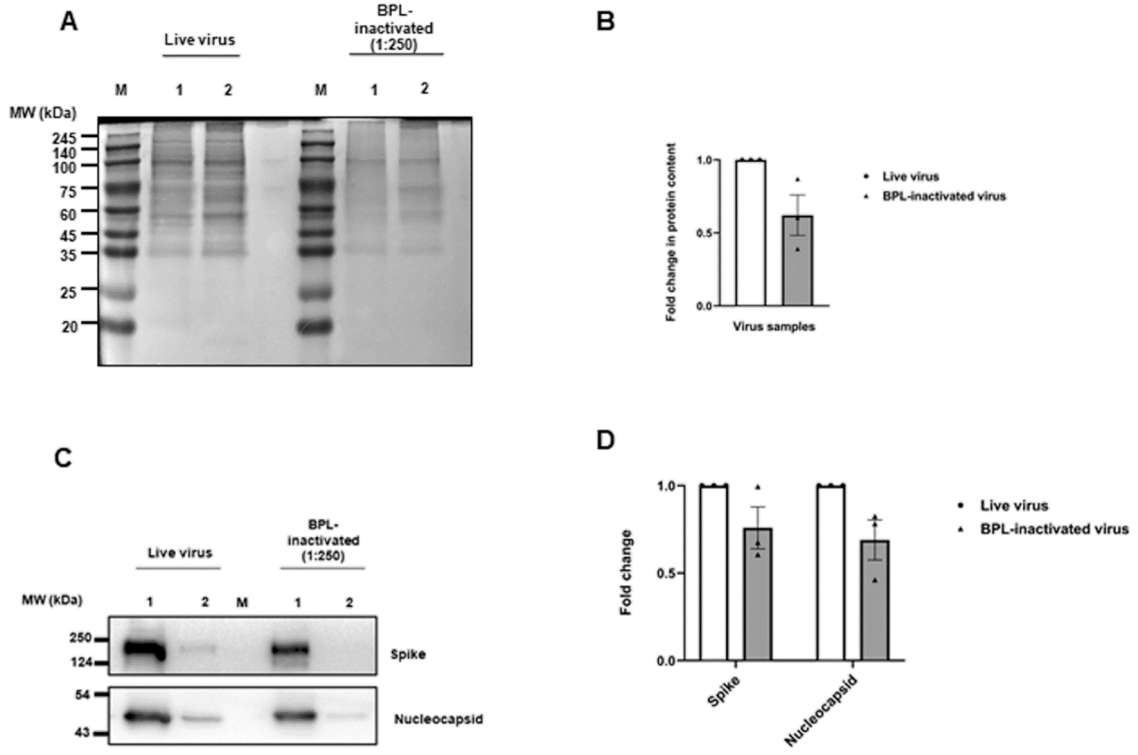

Fig. 3. Qualitative analysis of the BPL inactivated virus samples with the infectious control samples. (A) Zinc stain of SDS-PAGE with samples from two individual live infectious or their corresponding inactivated samples. M indicates protein molecular weight marker and the numbers indicate two individual samples. Inactivation was performed by BPL at 1:250 concentrations. The concentrated samples were lysed in equal volumes of 2 × protein lysis buffer, mixed with 6 × Laemmli buffer, boiled and loaded into the gels. After electrophoresis, the gels were stained following the instructions provided by the manufacturer. (B) Relative protein contents in the active and inactivated samples were represented after quantifying the band intensities by ImageLab software. (C) Immunoblots for SARS-CoV-2 Spike and Nucleocapsid proteins. Concentrated samples separated on SDS-PAGE were transferred onto PVDF membrane and subsequently immunoblotted using specific antibodies against the proteins. (D) Relative antigenic integrity in infectious and BPL inactivated virus samples. Immunoblot images were analyzed by ImageJ software for quantification.

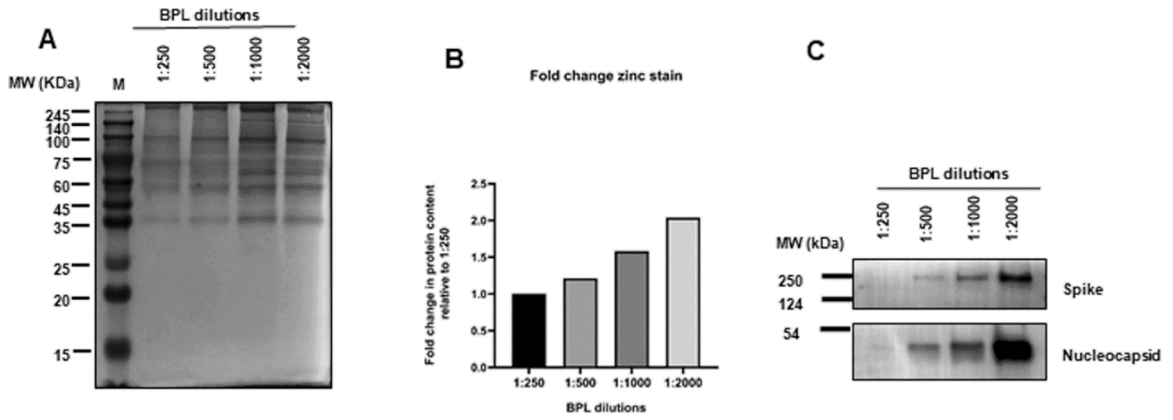

Fig. 4. Confirmation of the loss of antigenic integrity by BPL (A) Viral supernatants were treated with varying concentrations of BPL as mentioned in the figure and subsequently concentrated before separating on SDS-PAGE. As in Fig. 3A, the gel was zinc stained to visualize the protein bands. (B) Quantification of the intensities of protein bands in lanes representing the samples treated with the respective BPL concentrations. The raw intensities were normalized against that from the highest BPL concentration (1:250). (C) Immunoblotting of the viral proteins in samples treated with varying concentrations of BPL. Samples were separated on SDS-PAGE after which they were transferred onto PVDF membrane and immunoblotted.

immunogenicity of the prepared samples. We immunoblotted the infectious and inactivated SARS-CoV-2 supernatants for the presence of HSP90, GAPDH and β-actin. However, these proteins could not be detected in any of the viral samples (Fig. 5F). These results indicate that either the virions do not associate with host proteins or associate at sub-detectable levels and that such host proteins may not be associating with the virion aggregates during BPL inactivation. Increased aggregation of virions could result in significant loss in the exposure of the epitopes and hence would render them less suitable for antibody response. The possibility of such a consequence needs to be further studied. Additionally, filtration of the mixture post-BPL treatment is not advisable as it might cause significant loss of virion aggregates. Increased aggregation coupled with lower exposure of viral proteins indicates that higher concentrations of BPL are not optimal for production of vaccines.

4. Discussion

In this study, we focused on characterizing the methods for preparation of large volumes of inactivated SARS-CoV-2 cultures for therapeutic purposes such as vaccine and antisera production. Since BPL is the mode of choice for inactivation of several microbes, we optimized the concentration and studied the impact of the treatment on the epitopes and virus aggregation. We demonstrate that BPL at 1:2000 (v/v) dilutions in the culture supernatant is sufficient to totally inactivate the virus. Our studies suggest that higher BPL concentrations negatively impacts the antigenic potential of the virus thereby potentially affecting the immune response when used as antigens. However, lower concentration of BPL at 1:2000 had minimal impact on the antigenic integrity in comparison with higher concentration suggesting that at this concentration, antigenic response should be robust.

Since BPL treatment impacted the antigenic potential of S and N, we speculate that it must be causing chemical modifications of amino acids. Similar reports have been made in the case of influenza and coxsackie viruses (Fan et al., 2017; She et al., 2013) suggesting that BPL might be interfering with the integrity of the structural proteins of the virion. In agreement with this data, protein quantitation of the BPL treated viral samples always failed to show reproducible results. Highly sensitive BCA method detected proteins in the viral samples, albeit in highly irreproducible manner (data not shown). We demonstrate that viral proteins from such samples could be detected by the zinc negative staining in SDS-PAGE and could be used for relative quantitation.

Our study demonstrates a clear dichotomy between the Ct values and infectious viral count in any given stock. While the Ct values are representatives of the levels of viral RNA, the plaque assays are direct indicators of the infectivity of the stocks. Our studies demonstrate a lack of correlation between the Ct and PFU values, and a strong correlation between low Ct values and high viral antigens, pointing to the possibility of the presence of a large fraction of non-infectious virus particles in these samples. Having lower infectious titer may not necessarily be a deterrent for samples used in immunizations given that they have high antigenic content. Our results suggest that samples with low Ct and low infectious titers can therefore be used for immunization purposes provided they have good antigenic contents.

While cytopathic effect (CPE) is a clear indication of the viral replication, we observed that several cultures that harbored very high titer virus did not display a CPE during the early part of viral culturing. On the other hand, a few cultures that displayed CPE could not establish viral cultures. Therefore, it is important to monitor the presence of the virus in the supernatant by qRT-PCR. If the cultures do not display CPE, qRT-PCR could be optimally performed at a week from the time of infection.

Our finding on the aggregation of SARS CoV-2 particles has significance in the vaccine and antisera industry. Studies have reported an association between aggregation and loss of antigenicity (Kon et al., 2016; Desbat et al., 2011; Chen et al., 2015). Our studies also tested the association of common host proteins reported elsewhere to associate with virions, but could not detect them either in the infectious or in the inactivated viral samples. Another concern is the incomplete inactivation due to aggregation and the potential escape of virus from inactivation resulting in the presence of infectious viruses in vaccine with a potential for infection (Delrue et al., 2012). However, our studies could not detect any traces of infectious virus after three rounds of consecutive infections. Nevertheless, total inactivation is achieved even at 1:2000 concentrations and hence higher concentrations of BPL are well avoidable.

5. Conclusion

We have successfully established culturing of multiple isolates of SARS-CoV-2 from patient samples including the modified dry-swab method of collection. We optimized the optimal concentrations of BPL for complete inactivation of SARS-CoV-2. Our studies identified those concentrations of BPL higher than 1:1000 results in aggregation of viral particles and also loss in the antigenic potential of the sample. Our studies would provide a good guiding material for antisera and vaccine studies.

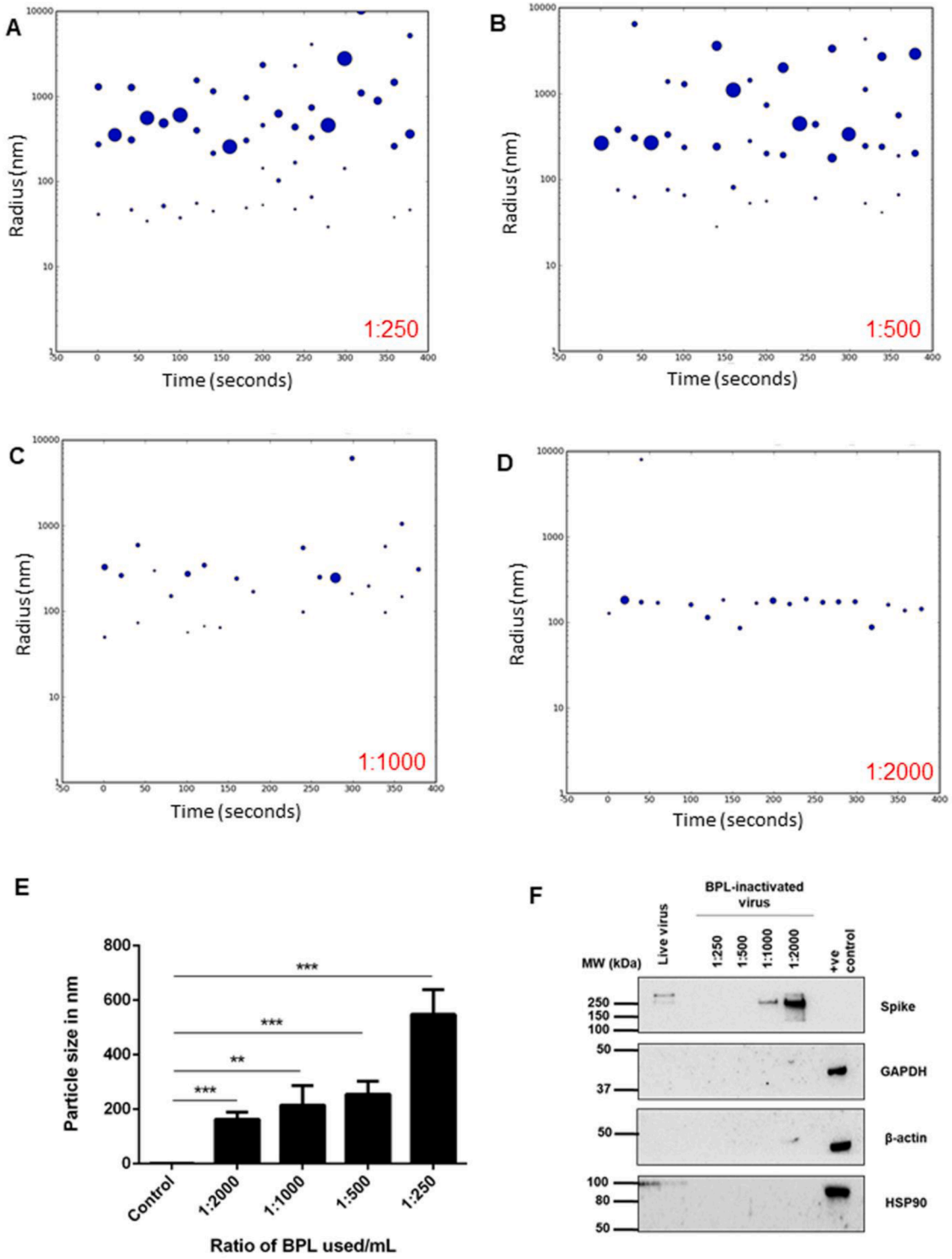

Fig. 5. BPL causes aggregation of SARS-CoV-2 particles. (A-D) Representative images of analysis of the particle size of SARS-CoV-2 inactivated with BPL at 1: 250, 1:500, 1:1000 and 1: 2000 concentrations (v/v) by dynamic light scattering. Serum-free culture medium was used as the control. (E) Average size of the virus particles treated with varying concentrations of BPL as mentioned. Error bars indicates SEM ($n = 3$). ***$p \leq 0.0005$; **$p \leq 0.005$; *$p \leq 0.05$. (F) Analysis of the presence of host proteins in the viral preparations by immunoblotting. The preparations were lysed in the lysis buffer before subjecting to SDS-PAGE. Total cellular lysates of A549 cells were used as positive control.

Author contributions

D.G. optimized large-scale SARS-CoV-2 virus propagation, BPL inactivation and plaque assay. D.G., and D.T. propagated, quantified and inactivated large-scale SARS-CoV-2 cultures and performed DLS experiments. D.V. and V.S. established SARS-CoV-2 cultures used in this study. H.P. performed immunoblotting. V.S. performed zinc staining. K. H.H. conceptualized the study and wrote the manuscript. Institutional ethics clearance: Institutional ethics clearance (IEC-82/2020) was obtained for the patient sample processing for virus culture. Institutional biosafety: Institutional biosafety clearance was obtained for the experiments pertaining to SARS-CoV-2.

Declaration of Competing Interest

The authors declare that they have no known competing financial interests or personal relationships that could have appeared to influence the work reported in this paper.

Acknowledgement

We thank several volunteers at the Center for Cellular and Molecular Biology, who were part of COVID-19 testing that helped us gain access to the potential patient samples for virus culturing. Special thanks to Amit Kumar and Mohan Singh Moodu for their help with the logistics. K Mallesham, R Rukmini helped with DLS experiments and analysis. We thank Karthika Nair, Abhirami P S, Sai Poojitha, and Soumya Bunk for their help with experiments.

Funding

The work was supported by the internal funding from CSIR-CCMB.

References

Lu, R., Zhao, X., Li, J., Niu, P., Yang, B., Wu, H., et al., 2020. Genomic characterisation and epidemiology of 2019 novel coronavirus: implications for virus origins and receptor binding. Lancet 395, 565–574.
Zhu, N., Zhang, D., Wang, W., Li, X., Yang, B., Song, J., et al., 2020. A novel coronavirus from patients with pneumonia in China, 2019. N. Engl. J. Med. 382, 727–733.
Puelles, V.G., Lütgehetmann, M., Lindenmeyer, M.T., Sperhake, J.P., Wong, M.N., Allweiss, L., et al., 2020. Multiorgan and renal tropism of SARS-CoV-2. N. Engl. J. Med. 383, 590–592.
Chen, H., Wu, R., Xing, Y., Du, Q., Xue, Z., Xi, Y., et al., 2020. Influence of different inactivation methods on severe acute respiratory syndrome coronavirus 2 RNA copy number. J. Clin. Microbiol. 58.
Furuya, Y., Chan, J., Regner, M., Lobigs, M., Koskinen, A., Kok, T., et al., 2010. Cytotoxic T cells are the predominant players providing cross-protective immunity induced by {gamma}-irradiated influenza a viruses. J. Virol. 84, 4212–4221.
Fan, C., Ye, X., Ku, Z., Kong, L., Liu, Q., Xu, C., et al., 2017. Beta-propiolactone inactivation of coxsackievirus A16 induces structural alteration and surface modification of viral capsids. J. Virol. 91.
Roberts, A., Lamirande, E.W., Vogel, L., Baras, B., Goossens, G., Knott, I., et al., 2010. Immunogenicity and protective efficacy in mice and hamsters of a β-propiolactone inactivated whole virus SARS-CoV vaccine. Viral Immunol. 23, 509–519.
Patterson, E.I., Prince, T., Anderson, E.R., Casas-Sanchez, A., Smith, S.L., Cansado-Utrilla, C., et al., 2020. Methods of inactivation of SARS-CoV-2 for downstream biological assays. J. Infect. Dis. 222, 1462–1467.
Jureka, A.S., Silvas, J.A., Basler, C.F., 2020. Propagation, inactivation, and safety testing of SARS-CoV-2. Viruses 12.
Kariwa, H., Fujii, N., Takashima, I., 2004. Inactivation of SARS coronavirus by means of povidone-iodine, physical conditions, and chemical reagents. Jpn. J. Vet. Res. 52, 105–112.
See, R.H., Petric, M., Lawrence, D.J., Mok, C.P.Y., Rowe, T., Zitzow, L.A., et al., 2008. Severe acute respiratory syndrome vaccine efficacy in ferrets: whole killed virus and adenovirus-vectored vaccines. J. Gen. Virol. 89, 2136–2146.
See, R.H., Zakhartchouk, A.N., Petric, M., Lawrence, D.J., Mok, C.P.Y., Hogan, R.J., et al., 2006. Comparative evaluation of two severe acute respiratory syndrome (SARS) vaccine candidates in mice challenged with SARS coronavirus. J. Gen. Virol. 87, 641–650.
Kempner, E.S., 2001. Effects of high-energy electrons and gamma rays directly on protein molecules. J. Pharm. Sci. 90, 1637–1646.
Kiran, U., Gokulan, C.G., Kuncha, S.K., Vedagiri, D., Chander, B.T., Sekhar, A.V., et al., 2020. Easing diagnosis and pushing the detection limits of SARS-CoV-2. Biol. Methods Protoc. 5, bpaa017.
George, A., Panda, S., Kudmulwar, D., Chhatbar, S.P., Nayak, S.C., Krishnan, H.H., 2012. Hepatitis C virus NS5A binds to the mRNA cap-binding eukaryotic translation initiation 4F (eIF4F) complex and up-regulates host translation initiation machinery through eIF4E-binding protein 1 inactivation. J. Biol. Chem. 287, 5042–5058.
Schneider, C.A., Rasband, W.S., Eliceiri, K.W., 2012. NIH Image to ImageJ: 25 years of image analysis. Nat. Methods 9, 671–675.
Kaye, M., 2006. SARS-associated coronavirus replication in cell lines. Emerg. Infect. Dis. 12, 128–133.
Stelzer-Braid, S., Walker, G.J., Aggarwal, A., Isaacs, S.R., Yeang, M., Naing, Z., et al., 2020. Virus isolation of severe acute respiratory syndrome coronavirus 2 (SARS-CoV-2) for diagnostic and research purposes. Pathology 52, 760–763.
Caly, L., Druce, J., Roberts, J., Bond, K., Tran, T., Kostecki, R., et al., 2020. Isolation and rapid sharing of the 2019 novel coronavirus (SARS-CoV-2) from the first patient diagnosed with COVID-19 in Australia. Med. J. Aust. 212, 459–462.
Díaz, F.J., Aguilar-Jiménez, W., Flórez-Álvarez, L., Valencia, G., Laiton-Donato, K., Franco-Muñoz, C., et al., 2020. Isolation and characterization of an early SARS-CoV-2 isolate from the 2020 epidemic in Medellín, Colombia. Biomed. Rev. Inst. Nac. Salud 40, 148–158.
Pujadas, E., Chaudhry, F., McBride, R., Richter, F., Zhao, S., Wajnberg, A., et al., 2020. SARS-CoV-2 viral load predicts COVID-19 mortality. Lancet Respir. Med. 8, e70.
Karahasan Yagci, A., Sarinoglu, R.C., Bilgin, H., Yanılmaz, Ö, Sayın, E., Deniz, G., et al., 2020. Relationship of the cycle threshold values of SARS-CoV-2 polymerase chain reaction and total severity score of computerized tomography in patients with COVID 19. Int. J. Infect. Dis. IJID Off. Publ. Int. Soc. Infect. Dis. 101, 160–166.
Borsanyiova, M., Kubascikova, L., Sarmirova, S., Vari, S.G., Bopegamage, S., 2018. Assessment of a swab collection method without virus transport medium for PCR diagnosis of coxsackievirus infections. J. Virol. Methods 254, 18–20.
Moore, C., Corden, S., Sinha, J., Jones, R., 2008. Dry cotton or flocked respiratory swabs as a simple collection technique for the molecular detection of respiratory viruses using real-time NASBA. J. Virol. Methods 153, 84–89.
La Scola, B., Le Bideau, M., Andreani, J., Hoang, V.T., Grimaldier, C., Colson, P., et al., 2020. Viral RNA load as determined by cell culture as a management tool for discharge of SARS-CoV-2 patients from infectious disease wards. Eur. J. Clin. Microbiol. Infect. Dis. Off. Publ. Eur. Soc. Clin. Microbiol. 39, 1059–1061.
Kim, S.E., Jeong, H.S., Yu, Y., Shin, S.U., Kim, S., Oh, T.H., et al., 2020. Viral kinetics of SARS-CoV-2 in asymptomatic carriers and presymptomatic patients. Int. J. Infect. Dis. IJID Off. Publ. Int. Soc. Infect. Dis. 95, 441–443.
Wiktor, T.J., Aaslestad, H.G., Kaplan, M.M., 1972. Immunogenicity of rabies virus inactivated by -propiolactone, acetylethyleneimine, and ionizing irradiation. Appl. Microbiol. 23, 914–918.
Logrippo, G.A., Hartman, F.W., 1955. Antigenicity of beta-propiolactone-inactivated virus vaccines. J. Immunol. 75, 123–128. Baltimore, Md: 1950.
Perrin, P., Morgeaux, S., 1995. Inactivation of DNA by beta-propiolactone. Biol. J. Int. Assoc. Biol. Stand. 23, 207–211.
Gale, T.V., Horton, T.M., Hoffmann, A.R., Branco, L.M., Garry, R.F., 2019. Host proteins identified in extracellular viral particles as targets for broad-spectrum antiviral inhibitors. J. Proteome Res. 18, 7–17.
She, Y.M., Cheng, K., Farnsworth, A., Li, X., Cyr, T.D., 2013. Surface modifications of influenza proteins upon virus inactivation by β-propiolactone. Proteomics 13, 3537–3547.
Kon, T.C., Onu, A., Berbecila, L., Lupulescu, E., Ghiorgisor, A., Kersten, G.F., et al., 2016. Influenza vaccine manufacturing: effect of inactivation, splitting and site of manufacturing. Comparison of influenza vaccine production processes. PLoS One 11, e0150700.
Desbat, B., Lancelot, E., Krell, T., Nicolaï, M.-C., Vogel, F., Chevalier, M., et al., 2011. Effect of the β-propiolactone treatment on the adsorption and fusion of influenza A/Brisbane/59/2007 and A/New Caledonia/20/1999 Virus H1N1 on a Dimyristoylphosphatidylcholine/Ganglioside GM3 mixed phospholipids monolayer at the air–water interface. Langmuir 27, 13675–13683.
Chen, Y., Zhang, Y., Quan, C., Luo, J., Yang, Y., Yu, M., et al., 2015. Aggregation and antigenicity of virus like particle in salt solution–a case study with hepatitis B surface antigen. Vaccine 33, 4300–4306.
Delrue, I., Verzele, D., Madder, A., Nauwynck, H.J., 2012. Inactivated virus vaccines from chemistry to prophylaxis: merits, risks and challenges. Expert Rev. Vaccines 11, 695–719.